



Communication

Biomimetic synthesis of all-inclusive organic-inorganic nanospheres for enhanced electrochemical immunoassay

Luyuan Tian^a, Yuxiao Ma^b, Ming Li^a, Qiaorong Tang^a, Luyang Miao^a, Bing Geng^{a,**}, He Li^{a,c,*}

^a School of Chemistry and Chemical Engineering and Institute of Surface Analysis and Chemical Biology, University of Jinan, Ji'nan 250022, China

^b The Hospital of University of Jinan, Ji'nan 250022, China

^c College of Optoelectronics Technology, Chengdu University of Information Technology, Chengdu 610225, China



ARTICLE INFO

Article history:

Received 25 July 2019

Received in revised form 7 October 2019

Accepted 9 October 2019

Available online 15 October 2019

Keywords:

Nuclear matrix protein 22

Biomimetic process

Electrochemical immunosensor

Limit of detection

ABSTRACT

A friendly biomimetic process was adopted for the mild preparation of “all-inclusive” organic-inorganic nanospheres, which effectively integrate biorecognition function and signal amplification function. The resulted $\text{Ca}_3(\text{PO}_4)_2\text{-Ab}_2\text{-BSA}$ nanospheres were employed as signal labels for enhancing detection of nuclear matrix protein 22 (NMP 22). The fabricated electrochemical immunosensor exhibited a linear range (0.08–77.00 U/mL) and an ultralow limit of detection (0.01 U/mL) towards NMP 22, which can be taken as a promising tool for clinical diagnosis of bladder cancer.

© 2019 Chinese Chemical Society and Institute of Materia Medica, Chinese Academy of Medical Sciences.

Published by Elsevier B.V. All rights reserved.

Bladder cancer (BC) is the second most common genitourinary malignancy [1]. Clinical diagnosis of BC has great meaning for the effective treatment of BC, cystoscopy has been the clinical standard for the identification of bladder cancer, while the relative high cost and invasive detection manner will bring heavy burden for BC patients [2,3]. Therefore, it is a high desire to develop sensitive, cost-effective and noninvasive methods for the detection of BC. Nuclear matrix protein 22 (NMP 22) as a tumor marker has been approved by US Food and Drug Administration for clinical diagnosis of BC and the clinical judgment value in urine was 10 U/mL, and if the value was higher than 10 U/mL, the detection results were positive [4].

Accordingly, some methods have been developed for sensitive detection of NMP 22, such as fluorescent, colorimetric [5], electrochemiluminescence [6], electrochemical [7–12]. Benefit from the advantages of low cost, friendly operation, rapid readout and satisfied sensitivity, electrochemical methodology has become a welcome method for tumor diagnosis beyond BC detection [13]. It is well worth to mention that some excited advancements have been made using nanomaterials to enhance the sensitivity of

electrochemical immunoassay for protein biomarkers, which offer more accurate cancer diagnosis [14].

Recently, extensive efforts have been made to prepare “all-inclusive” or “all-in-one” nanomaterials for biomedical applications [15–19]. “All-in-one” nanomaterials can integrate diagnostic component and therapeutic component into one single unit, which will be an ideal platform for healthcare. Moreover, “all-in-one” nanomaterials combining recognition function and signal amplification function do favor for sensing and biosensing applications.

Inspired by the mentioned work, we proposed a facile biomineralization method to prepare a novel kind of “all-inclusive” organic-inorganic nanospheres, $\text{Ca}_3(\text{PO}_4)_2\text{-Ab}_2\text{-BSA}$, as signal labels (Fig. 1A). $\text{Ca}_3(\text{PO}_4)_2\text{-Ab}_2\text{-BSA}$ nanospheres possess the unique features: Ab_2 will play biorecognition function for target analytes, BSA will diminish the non-specific adsorption and the inorganic component of $\text{Ca}_3(\text{PO}_4)_2$ can supply plenty of phosphate ions to react with molybdate ions in acid medium to produce a large amount of redox-active molybdophosphates, which is the origin of the detection electrochemical signal. Much more produced molybdophosphates can significantly amplify the detection signal of the electrochemical immunoassay. Herein, we fabricated a “sandwich” type electrochemical immunosensor for bladder cancer using $\text{Ca}_3(\text{PO}_4)_2\text{-Ab}_2\text{-BSA}$ as signal labels. As demonstrated in Fig. 1B, carboxylated single-wall carbon nanotubes (CNT) were used as a substrate material to increase conductivity. After the sandwich type immunoreactions were finished, the following reaction of “all-inclusive” $\text{Ca}_3(\text{PO}_4)_2\text{-Ab}_2\text{-BSA}$ nanospheres with molybdate will

* Corresponding author at: School of Chemistry and Chemical Engineering, and Institute of Surface Analysis and Chemical Biology, University of Jinan, Ji'nan, 250022, China.

** Corresponding author.

E-mail addresses: chm_gengb@ujn.edu.cn (B. Geng), lihecd@gmail.com (L. He).

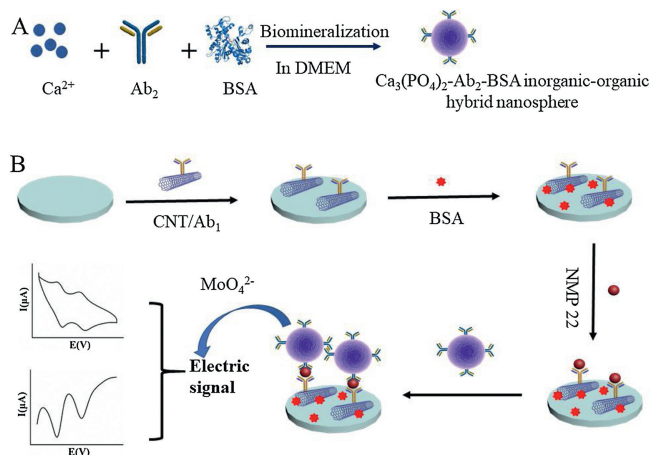


Fig. 1. Schematic illustration of the synthesis procedure of $\text{Ca}_3(\text{PO}_4)_2\text{-Ab}_2\text{-BSA}$ hybrid nanospheres as signal labels (a) and the established process of the electrochemical immunoassay for NMP 22 detection (b).

generate electrochemical current which is relation to the concentrations of NMP 22.

To our best knowledge, Ab_2 , as protein, contain some acidic amino acid residues which can chelate calcium ions, and then providing nucleation sites [20]. Nanoscale calcium phosphate crystals were constantly generated around the periphery of the peptide through spontaneous nucleation, and according to the bricks-and-mortar self-assembly mechanism, organized spherical structures was formed [21]. The morphology of the as-synthesized $\text{Ca}_3(\text{PO}_4)_2\text{-Ab}_2\text{-BSA}$ were recorded by transmission electron microscopy (TEM). As illustrated by the SEM image in Fig. 2a, the $\text{Ca}_3(\text{PO}_4)_2$ nanoparticles showed spherical structure with a diameter around 200 nm. The TEM image (Fig. 2b) of the $\text{Ca}_3(\text{PO}_4)_2$ also exhibited typical spherical structure. The XRD pattern (Fig. 2c) of the calcium phosphate nanospheres was well-indexed to $\text{Ca}_3(\text{PO}_4)_2 \cdot x\text{H}_2\text{O}$ (JCPDS card No. 18-0303). The first decline before 200°C was contributed to the decreased of H_2O and the content of H_2O was about 7.2 wt%. And the organic components including BSA and Ab_2 decomposed from 200°C to 800°C , the content

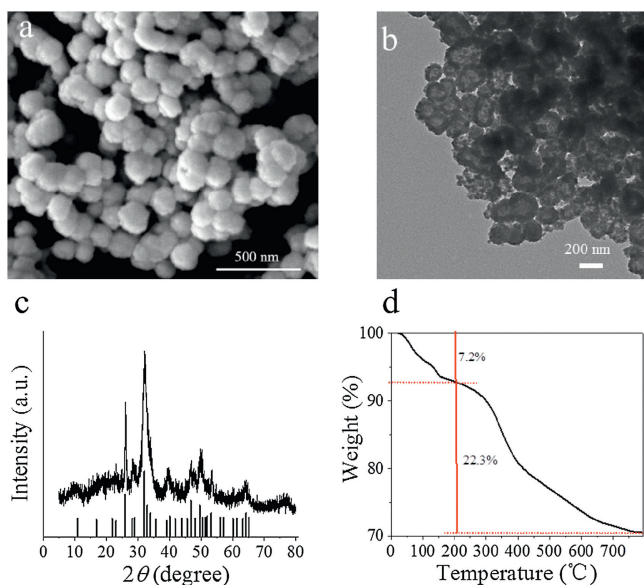


Fig. 2. (a) SEM image, (b) TEM image, (c) X-ray diffraction patterns and (d) TGA analysis of $\text{Ca}_3(\text{PO}_4)_2\text{-Ab}_2\text{-BSA}$ nanospheres.

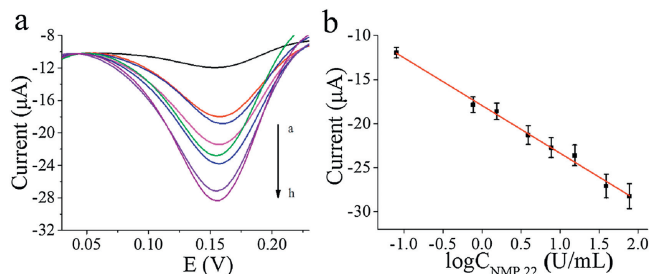


Fig. 3. (a) SWV responses of the fabricated electrochemical immunosensor towards various concentrations of NMP 22 (from a to h, 0.08, 0.77, 1.54, 3.90, 7.70, 15.40, 39.00 and 77.00 U/mL); (b) Calibration curve of the immunosensor towards NMP 22. Error bar = RSD ($n = 5$).

was around 22.3 wt% and the residual substance was $\text{Ca}_3(\text{PO}_4)_2$ (Fig. 2d).

A series of electrochemical immunosensors were developed for detecting different concentrations of NMP 22. Under the optimized conditions (Fig. S4 in Supporting information), the concentrations of NMP 22 were correlation with the SWV peak currents at 0.16 V (Fig. 3a). Importantly, the electrochemical immunosensor presents a sensitive detection performance toward NMP 22 which has a relationship with the logarithm of the NMP 22 concentration, ranging from 0.08 U/mL to 77.00 U/mL. Moreover, the calibration curve of the developed immunosensor was $I (\mu\text{A}) = -17.95 - 5.40 \log C_{\text{NMP 22}} (\text{U/mL})$ ($R^2 = 0.994$), as shown in Fig. 3b and the detect limit was 0.01 U/mL ($S/N = 3$).

Meanwhile, the established electrochemical immunosensor possessed excellent reproducibility and good stability for the detection of NMP 22 (Fig. S5 in Supporting information). In order to assess the application potential and reliability of this immunosensor for real sample analysis, five urine samples (Numbering them as 1, 2, 3, 4, 5. Among of them, samples 1, 4 and 5 are negative, the other two are positive) diluted 100 times were conducted for further evaluation. As shown in Table S1 (Supporting information), the results matched well with the actual states of samples. Thus, the immunosensor is promising for clinical determination of NMP 22.

In summary, a satisfied sandwich electrochemical immunosensor was developed for NMP 22 detection. The good performance of the immunosensor was attributed to the promoted electrons transfer owing to the good conductivity of CNT and the amplified detection current signal by the transformation from $\text{Ca}_3(\text{PO}_4)_2$ to redox-active molybdophosphates.

Declaration of competing interest

The authors declare that they have no known competing financial interests or personal relationships that could have appeared to influence the work reported in this paper.

Acknowledgments

This work was supported by the Natural Science Foundation of Shandong Province (No. ZR2017MB017). We also gratefully acknowledge the support from the One-Thousand-Talents Scheme in Sichuan Province.

References

- [1] D.S. Stampfer, G.A. Carpinito, J. Rodriguez-Villanueva, et al., *J. Urol.* 159 (1998) 394–398.
- [2] M.F. Botteman, C.L. Pashos, A. Redaelli, B. Laskin, R. Hauser, *PharmacoEconomics* 21 (2003) 1315–1330.
- [3] E.C. Hwang, H.S. Choi, D.D. Kwon, et al., *Urology* 77 (2011) 154–159.

- [4] C. Zippe, L. Pandrangi, A. Agarwal, *J. Urol.* 161 (1999) 62–65.
- [5] X.F. Tan, H. Li, G.X. Zheng, et al., *Chin. Chem. Lett.* 30 (2019) 1307–1309.
- [6] T.Q. Han, D. Wu, B. Du, et al., *Sens. Actuators B-Chem.* 205 (2014) 176–183.
- [7] M.H. Lee, Y.C. Thomas, B.D. Liu, et al., *Biosens. Bioelectron.* 79 (2016) 789–795.
- [8] X. Ren, H.M. Ma, B. Du, et al., *ACS Appl. Mater. Interfaces* 43 (2017) 37637–37644.
- [9] S.Y. Li, S. Yue, Q.B. Yu, et al., *Analyst* 144 (2019) 649–655.
- [10] G.W. Wang, H. Wang, S. Cao, et al., *Microchim. Acta* 186 (2019) 96.
- [11] G.J. Yang, C.L. Tang, Y. Deng, et al., *Chin. Chem. Lett.* 29 (2018) 1857–1860.
- [12] X.Y. Lin, T.X. Lan, Y.N. Ni, et al., *Chin. Chem. Lett.* 30 (2019) 1157–1160.
- [13] N.Y. Morgan, H.S. Eden, X.Y. Chen, et al., *ACS Nano* 8 (2012) 6546–6561.
- [14] A.C. Chen, S.H. Chatterjee, *Chem. Soc. Rev.* 42 (2013) 5425–5438.
- [15] J. Ge, J.D. Lei, R.N. Zare, *Nature Nanotech.* 7 (2012) 428–432.
- [16] Y. Liu, W.Y. Zhen, Y.H. Wang, J.H. Liu, H.J. Zhang, *ACS Nano* 12 (2018) 4886–4893.
- [17] G.X. Lv, W.S. Guo, P.C. Wang, et al., *ACS Nano* 10 (2016) 9637–9645.
- [18] H.C. Yan, W.S. Liu, Y. Tang, et al., *Anal. Chem.* 8 (2019) 5225–5234.
- [19] Q.R. Tang, L.H. Zhang, Q. Wei, et al., *Biosens. Bioelectron.* 133 (2019) 94–99.
- [20] S. Mann, *Nature* 365 (1995) 499–505.
- [21] A.K. Boal, J.E. Derouchey, T.T. Albrecht, et al., *Nature* 404 (2000) 746–748.